

Cite this: *Green Chem.*, 2014, **16**, 3255

A sustainable route to produce the scytonemin precursor using *Escherichia coli*[†]

Sailesh Malla^a and Morten O. A. Sommer^{*a,b}

Scytonemin is an indolic-phenolic natural product with potent pharmaceutical activities and possible application as a sunscreen. However, the productivity of the existing synthesis systems restrains its applications in medicine and cosmetics. In this paper, we report the generation of the monomer moiety of scytonemin from tryptophan and tyrosine in *Escherichia coli*. We heterologously expressed the biosynthetic pathway from *Nostoc punctiforme* and discovered that only three enzymes from *N. punctiforme* are required for the *in vivo* production of the monomer moiety of scytonemin in *E. coli*. We also found that the constructed recombinant *E. coli* strains are capable of producing novel alkaloids as shunt products. The recombinant *E. coli* strain expressing the putative scytonemin biosynthetic gene cluster produced 4.2 mg L^{-1} ($2.46 \text{ }\mu\text{g mg}^{-1}$ dry cell weight) of the monomer moiety of scytonemin without supplementation of extracellular substrates whereas upon supplementation with 1 mM of the substrates to the *E. coli* strain harboring *scyABC* genes, 8.9 mg L^{-1} ($4.56 \text{ }\mu\text{g mg}^{-1}$ dry cell weight) of the monomer moiety of scytonemin was produced in 5 days. Combining this cell factory with the previously described chemical dimerization process will contribute to a sustainable production of semi-synthetic scytonemin.

Received 22nd January 2014,
Accepted 1st April 2014

DOI: 10.1039/c4gc00118d
www.rsc.org/greenchem

Introduction

Alkaloids, a diverse group of nitrogen-containing natural products, are produced by a large variety of organisms including bacteria, fungi, insects, plants and animals. Numerous alkaloids are pharmacologically well characterized and are used as clinical drugs, ranging from chemotherapeutics to analgesic agents.¹ Studies on plant alkaloids suggest that they are involved in the defense mechanism against herbivores, insects and pathogens.² Since alkaloids are toxic, they are usually produced in small quantities by their native producer organisms. Scytonemin is an alkaloid pigment consisting of a symmetrical dimeric carbon skeleton composed of fused heterocyclic units with conjugated double-bond distribution (Fig. 1) synthesized by numerous cyanobacteria.³ Scytonemin is the first described small molecule that inhibits human polo-like kinase 1 (PLK1).⁴ PLK1 has multiple functions during mitosis and plays a significant role in maintaining the genomic stability.⁵ Furthermore, PLK1 is highly expressed in a broad spectrum of cancer cells, indicating its possibility of being involved in carcinogenesis.⁶ Scytonemin (at $3\text{--}4 \text{ }\mu\text{M}$ concentration) can

inhibit cell growth by cell cycle arrest in multiple myeloma cells and renal cancer cells through specific down-regulation of the PLK1 activity.^{7,8} Scytonemin is not cytotoxic (up to $10 \text{ }\mu\text{M}$) to non-proliferating cells, highlighting its possible application in medicine.^{9,10} In addition to kinase inhibitory activities, scytonemin also acts as a natural microbial sunscreen by effectively minimizing cellular damage caused by UV ($315\text{--}400 \text{ nm}$) exposure.¹¹ Scytonemin also exhibits a radical-scavenging activity¹² and its synthesis was enhanced by oxidative stress in cyanobacteria.¹³

The putative scytonemin biosynthetic gene cluster from *Nostoc punctiforme* ATCC 29133 consists of 18 unidirectional open reading frames (*orfs*) (Fig. 2). Native expression of this gene cluster is triggered by exposure to UV light, resulting in extracellular pigment accumulation. Once scytonemin has reached sufficient quantities in the extracellular slime layer to block the incoming UVA, the gene expression returns to background levels and halts further scytonemin synthesis.^{14,15} Due to the potent UV light absorption of scytonemin, the accumulated scytonemin concentration is low ($\sim 1.3 \text{ }\mu\text{g mg}^{-1}$ of dry cell weight (DCW)) in currently characterized cyanobacterial strains under laboratory culture conditions¹⁶ whereas naturally growing colonies of a terrestrial cyanobacterium *N. commune* contained only $0.4 \text{ }\mu\text{g mg}^{-1}$ of DCW of scytonemin.¹⁷ Consequently, direct extraction from natural producers is unfeasible on a large scale. Another route to produce scytonemin is through chemical synthesis. The total synthesis of scytonemin has been reported from 3-indole acetic acid through a process

^aThe Novo Nordisk Foundation Center for Biosustainability, Technical University of Denmark, DK-2970 Hørsholm, Denmark

^bDepartment of Systems Biology, Technical University of Denmark, DK-2800 Lyngby, Denmark. E-mail: msom@bio.dtu.dk

† Electronic supplementary information (ESI) available. See DOI: [10.1039/c4gc00118d](https://doi.org/10.1039/c4gc00118d)



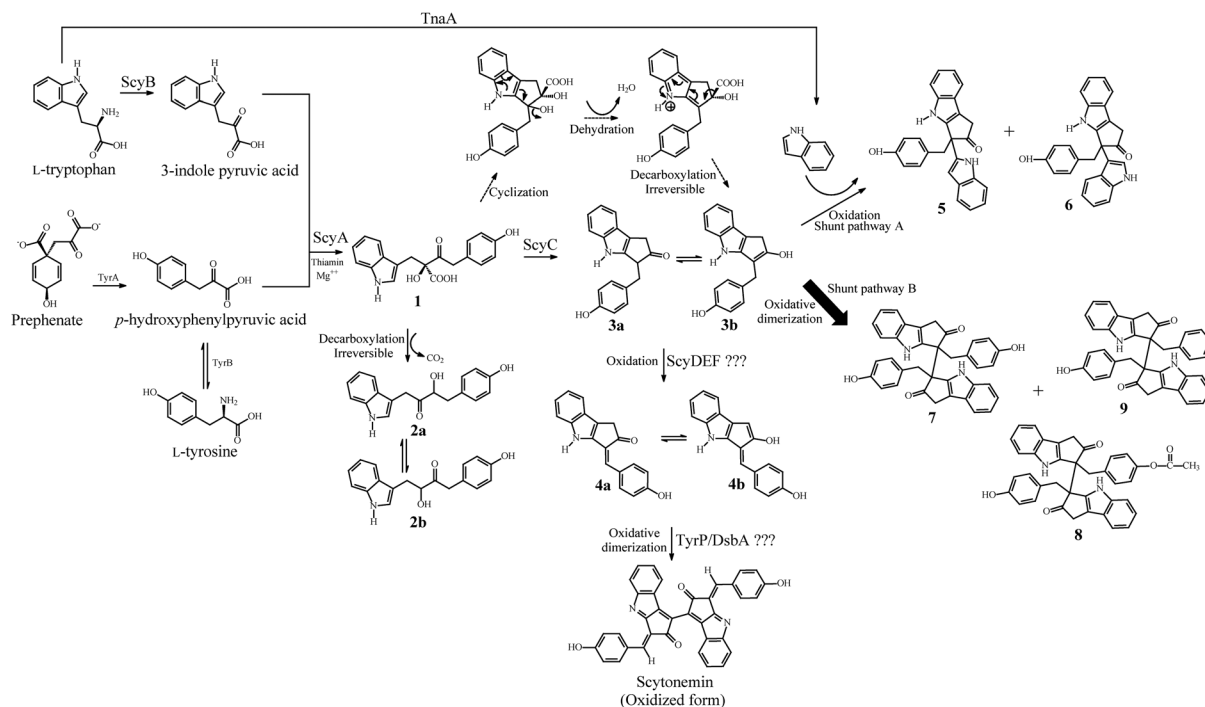


Fig. 1 Proposed biosynthetic pathway for scytonemin and the competing shunt pathways A and B in *E. coli*. The shunt pathways A and B produced new alkaloid derivatives.

comprising nine chemical steps resulting in approximately 4% conversion to the final product.¹⁸ Accordingly, more effective approaches are desired for the continuous, rapid and cost effective production of scytonemin.

Microbial cell factories offer extensive opportunities for the industrial production of complex biomolecules for cost effective biological synthesis.^{19–22} Furthermore, microbial fermentation often reduces the need for energy intensive reaction conditions, toxic organic solvents, heavy metal catalysts, and strong acids/bases, which are widely utilized in chemical synthesis routes.²³ Among the microbial cell factories designed, the Gram-negative bacterium *Escherichia coli* has become one of the most promising hosts, with a highly tractable genetic system and favorable fermentation conditions for production purposes.^{24–26} Indeed, plant based alkaloid compounds have been successfully produced from the engineered *E. coli* strains. For example, 46 mg L⁻¹ of the plant benzylisoquinoline alkaloid, (*S*)-reticuline, is produced from fermentation of metabolically engineered *E. coli* by utilizing simple carbon sources such as glucose or glycerol.¹⁹ Similarly, production of indole, a signaling molecule, from exogenous tryptophan in *E. coli* has been extensively studied.²⁷ Yields up to 6 mM of indole have been achieved from *E. coli* by supplementation of enough tryptophan in culture media.²⁸ In the present study, we described the construction of an *E. coli* cell factory for bio-based production of the key pharmaceutical intermediate, the monomer moiety of scytonemin (compound 4 in Fig. 1).

Materials and methods

Bacterial strains, plasmids, cultured conditions and chemicals

All strains, vectors and plasmids used in this study are listed in Table 1. All DNA manipulations were carried out by following standard protocols.²⁹ *E. coli* strains were routinely cultured in Luria–Bertani (LB) broth or on agar supplemented with the appropriate amount of antibiotics (ampicillin 100 µg mL⁻¹, chloramphenicol 25 µg mL⁻¹, streptomycin–spectinomycin 50 µg mL⁻¹ and kanamycin 35 µg mL⁻¹) when necessary. M9 minimal medium was used for production of intermediates and derivatives of scytonemin. All chemicals were purchased from Sigma-Aldrich (St. Louis, MO, USA). Restriction enzymes and T4 DNA ligase were purchased from New England Biolabs (Hertfordshire, UK) and Fermentas (Denmark). The DNA sequence was determined on an automated DNA sequence analyzer. The authentic scytonemin standard was kindly provided by Professor Jerker Mårtensson (Chalmers University of Technology, Sweden).

Plasmid construction

The construction of recombinant plasmids pCDF-ScyA, pCDF-ScyAC, pCDF-ScyACD, pACYC-ScyB, pET-ScyEF, pRSF-TyrP-DsbA, pC-ScyABC-ScyDEF, pE-GtAroB-TrpEC and pA-TrpAB-TrpDU is described below. All PCR primers used in this study are described in Table 2.

Based on pCDF-Duet-1, the expression recombinant plasmid pCDF-ScyACD was constructed, which allowed the



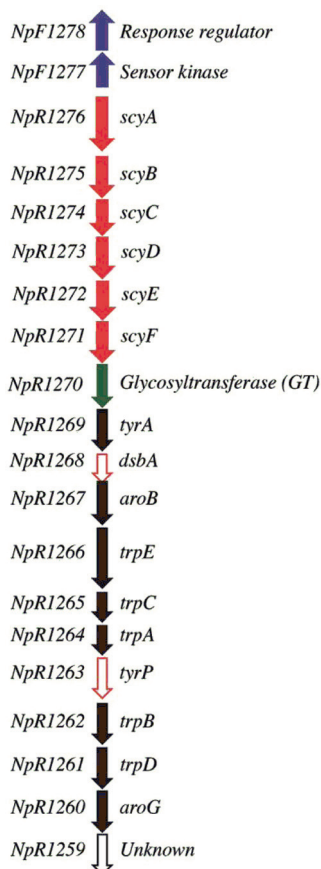


Fig. 2 Putative scytonemin biosynthetic gene cluster in ATCC 29133 (adapted from Soule *et al.*, 2009). Arrows represent genes and their transcriptional orientation. Blue filled arrow, regulatory gene; red filled arrow, core structural biosynthetic gene; red open arrow, anticipated core biosynthetic gene for final dimerization step; green filled arrow, glycosyltransferase; black filled arrow, aromatic amino acid biosynthetic gene; and black open arrow, unknown function.

simultaneous expression of the thiamin diphosphate (ThDP) dependent enzyme acetolactate synthase homologue, ScyA, (NpR1276, Genbank accession no. YP_001864940), ScyC (NpR1274, Genbank accession no. YP_001864938), and ScyD (NpR1273, Genbank accession no. YP_001864937) from *Nostoc punctiforme* ATCC 29133 in *E. coli*. Primer pairs ScyA_F/ScyA_R, ScyC_F/ScyC_R and ScyD_F/ScyD_R were used for the amplification of nucleotide sequences of *scyA* (1875 bp), *scyC* (969 bp) and *scyD* (1272 bp), respectively, from the genomic DNA of *N. punctiforme*. The PCR product of *scyA* was cloned into the *NcoI/BamHI* (MCS1) sites of pCDF-Duet-1 to construct the pCDF-ScyA recombinant expression plasmid. Similarly, the PCR product of *scyC* was cloned into the *NdeI/BglII* (MCS2) of the pCDF-ScyA plasmid to get the pCDF-ScyAC recombinant plasmid. The PCR product of *scyD* was cloned into the *NdeI/KpnI* (MCS2) of pCDF-Duet-1 vector to construct the pCDF-ScyD recombinant plasmid. Finally, using the primer pair ScyD_F_BglII/ScyD_R and pCDF-ScyD as a template, PCR was performed which allowed the amplification of the T7lac sequence along with the *scyD* structural gene. The PCR product,

T7-rbs-*ScyD*, was then cloned into the *BglII/KpnI* sites of pCDF-ScyAC to create the pCDF-ScyACD recombinant plasmid.

The primer pair ScyB_F/ScyB_R was used for the amplification of the leucine dehydrogenase homologue, ScyB (NpR1275, Genbank accession no YP_001864939), from *N. punctiforme* ATCC 29133 and the PCR product was cloned into pACYC-Duet-1 in *NcoI/BamHI* sites to construct the pACYC-ScyB expression recombinant plasmid.

Similarly, the primer pairs ScyE_F/ScyE_R and ScyF_F/ScyF_R were used to amplify *scyE* (NpR1272, Genbank accession no. YP_001864936) and *scyF* (NpR1271, Genbank accession no. YP_001864935) from the genomic DNA of *N. punctiforme*, respectively. The PCR product of *scyE* was cloned into pET-Duet-1 in *NcoI/BamHI* sites to construct the pET-ScyE expression recombinant plasmid. Furthermore, the PCR product of *scyF* was cloned into pRSF-ScyE excised with *NdeI/BglII* sites to construct the pET-ScyEF expression recombinant plasmid.

Likewise, the primer pairs TyrP_F/TyrP_R and DsbA_F/DsbA_R were used to amplify TyrP (NpR1263, Genbank accession no. YP_001864927) and DsbA (NpR1268, Genbank accession no. YP_001864932) from the genomic DNA of *N. punctiforme*, respectively. The PCR products of *tyrP* and *dsbA* were consecutively cloned into *NcoI/BamHI* and *NdeI/BglII* sites of pRSF-Duet-1 vector to construct the pRSF-TyrP-DsbA expression recombinant plasmid.

To express the putative scytonemin gene cluster (Fig. 2), recombinant plasmids pC-ScyABC-ScyDEF, pE-GTAroB-TrpEC and pA-TrpAB-TrpDU were constructed based upon pCDF-Duet-1, pET-Duet-1 and pACYC-Duet-1 expression vectors, respectively. The primer pairs ScyA_F/ScyC_R_BamHI, ScyD_F/ScyF_R, GT-AroB_F/GT-AroB_R, TrpEC_F/TrpEC_R, TrpAB_F/TrpAB_R, and TrpDU_F/TrpDU_R were used for amplification of *scyABC*, *scyDEF*, *Gt-tyrA-dsbA-aroB*, *trpE-trpC*, *trpA-tyrP-trpB*, and *trpD-aroG-NpR1259* regions of the putative scytonemin gene cluster from the genomic DNA of *N. punctiforme*, respectively. The PCR product of *scyABC* was cloned into the *NcoI/BamHI* (MCS1) sites of pCDF-Duet-1 to construct the pC-ScyABC recombinant expression plasmid. Further, the PCR product of *scyDEF* was cloned into the *NdeI/BglII* (MCS2) of the pC-ScyABC plasmid to construct pC-ScyABC-ScyDEF. Similarly, the PCR products of *Gt-tyrA-dsbA-aroB* and *trpE-trpC* were cloned into *NcoI/BamHI* (MCS1) and *NdeI/BglII* (MCS2) of pET-Duet-1 vector, respectively, to construct the pE-GtAroB-TrpEC recombinant plasmid. Finally, the PCR products of *trpA-tyrP-trpB* and *trpD-aroG-NpR1259* were cloned into *NcoI/BamHI* (MCS1) and *NdeI/BglII* (MCS2) of the pACYC-Duet-1 vector, respectively, to construct the pA-TrpAB-TrpDU recombinant plasmid.

In all cases, construction of recombinant plasmids was verified by both restriction mapping and direct nucleotide sequencing of respective genes in the recombinant plasmids.

Recombinant protein expression, whole-cell biotransformation, product isolation and determination of biomass

E. coli BL21(DE3) harboring recombinant plasmids were pre-cultured into 3 mL of LB liquid media with appropriate anti-



Table 1 Bacterial strains and plasmids used in this study

Strains/plasmids	Description	Source/reference
Strains		
<i>Escherichia coli</i>		
DH5 α	General cloning host	Invitrogen
BL21(DE3)	<i>ompT hsdT hsdS</i> ($r_B^- m_B^-$) <i>gal</i> (DE3)	Novagen
SM1	BL21(DE3) carrying pCDF-ScyA and pACYC-ScyB	This study
SM2	BL21(DE3) carrying pCDF-ScyAC and pACYC-ScyB	This study
SM3	BL21(DE3) carrying pCDF-ScyACD, pACYC-ScyB and pET-ScyEF	This study
SM4	BL21(DE3) carrying pCDF-ScyACD, pACYC-ScyB, pET-ScyEF and pRSF-tyrP-dsbA	This study
STN	BL21(DE3) carrying pC-ScyABC-ScyDEF, pE-GtAroB-TrpEC and pA-TrpAB-TrpDU	This study
Plasmids and vectors		
pET-Duet-1	Double T7 promoters, ColE1 ori, Amp ^r	Novagen
pCDF-Duet-1	Double T7 promoters, CloDF13 ori, Sm ^r	Novagen
pRSF-Duet-1	Double T7 promoters, RSF ori, Km ^r	Novagen
pACYC-Duet-1	Double T7 promoters, P15A ori, Cm ^r	Novagen
pCDF-ScyA	pCDF-Duet-1 carrying <i>scyA</i> from <i>Nostoc punctiforme</i>	This study
pCDF-ScyAC	pCDF-Duet-1 carrying <i>scyA</i> and <i>scyC</i> from <i>N. punctiforme</i>	This study
pCDF-ScyACD	pCDF-Duet-1 carrying <i>scyA</i> , <i>scyC</i> and <i>scyD</i> from <i>N. punctiforme</i>	This study
pACYC-ScyB	pACYC-Duet-1 carrying <i>scyB</i> from <i>N. punctiforme</i>	This study
pET-ScyEF	pET-Duet-1 carrying <i>scyE</i> and <i>scyF</i> from <i>N. punctiforme</i>	This study
pRSF-TyrP-DsbA	pRSF-Duet-1 carrying <i>tyrP</i> and <i>dsbA</i> from <i>N. punctiforme</i>	This study
pC-ScyABC-ScyDEF	pCDF-Duet-1 carrying <i>scyABC</i> and <i>scyDEF</i> from <i>N. punctiforme</i>	This study
pE-GtAroB-TrpEC	pET-Duet-1 carrying <i>Gt-tyrA-dsbA-aroB</i> and <i>trpE-trpC</i> from <i>N. punctiforme</i>	This study
pA-TrpAB-TrpDU	pACYC-Duet-1 carrying <i>trpA-tyrP-trpB</i> and <i>trpD-aroG-Npr1259</i> from <i>N. punctiforme</i>	This study

Table 2 Oligonucleotides used in this study^a

Primers	Oligonucleotide sequences (5'-3')	Restriction site
ScyA_F	TACCATGGGCATGAGTCAAAATATACTGGT	<i>Nco</i> I
ScyA_R	<u>TTCGGATC</u> CTAAACCATGGAAATGAAAC	<i>Bam</i> HI
ScyB_F	TACCATGGGCATGCTGCTATTGAAACTGTT	<i>Nco</i> I
ScyB_R	<u>TCGGATC</u> TTAACGCTGCGATCGCTTATAG	<i>Bam</i> HI
ScyC_F	ATAC <u>ATATGG</u> AAAAAAACTTTGCAACA	<i>Nde</i> I
ScyC_R	<u>TTGAGATC</u> TTAGTTGGGAACTAGGGATTC	<i>Bgl</i> II
ScyC_R_BamHI	<u>TTGGGATC</u> TTAGTTGGGAACTAGGGATTC	<i>Bam</i> HI
ScyD_F	ATAC <u>ATATG</u> AAACTGAAGCCATTCACTATT	<i>Nde</i> I
ScyD_R	<u>GAGGGTAC</u> CTTAGTTGAGATTATGGGAGGTG	<i>Kpn</i> I
ScyD_F_BglII	<u>GTAGATC</u> TATTGACACGGCCGCTAAAT	<i>Bgl</i> II
ScyE_F	TACCATGGGCATGAAACTCAAATCACTTACT	<i>Nco</i> I
ScyE_R	<u>TTCGGATC</u> TTAGACAGTCTCTGCTTCAC	<i>Bam</i> HI
ScyF_F	ATAC <u>ATATGG</u> ATTAGTCAAAATTGTCAA	<i>Nde</i> I
ScyF_R	<u>TTGAGATC</u> TCAGCATTGCTTTGCAGTTTC	<i>Bgl</i> II
TyrP_F	TACCATGGGCATGAAACTCCTGCTAAATC	<i>Nco</i> I
TyrP_R	<u>TTGGATC</u> TCATCTTGCCTTTCTTTTC	<i>Bam</i> HI
DsbA_F	ATAC <u>ATATG</u> CTAATAGATATCTTCATGATA	<i>Nde</i> I
DsbA_R	<u>TTGAGATC</u> TCATATTTCGCGGTATATC	<i>Bgl</i> II
GT-AroB_F	<u>TCCATGGG</u> CATGCAAATTCTGATTTATTCTCAT	<i>Nco</i> I
GT-AroB_R	<u>CCTGGATC</u> CCCTAAATTCCCTGCAATAGTGA	<i>Bam</i> HI
TrpEC_F	TTACATATGATTTAATTCCGTTCCTAC	<i>Nde</i> I
TrpEC_R	<u>GTCAGATC</u> CTAAAGAAAGCCTTAAAGACT	<i>Bgl</i> II
TrpAB_F	<u>TCCATGGG</u> CATGACCTCTATCTCAAATTCC	<i>Nco</i> I
TrpAB_R	<u>ACAGGATC</u> TTAAGGAATCAGGACTTGGC	<i>Bam</i> HI
TrpDU_F	<u>CTACATATG</u> ATAGCTGTAACCAAACATCGG	<i>Nde</i> I
TrpDU_R	<u>TATAGATC</u> TTCAAGAACGGATTAACATCGG	<i>Bgl</i> II

^a Restriction sites are indicated by underline and *italics*.

biotics and incubated at 37 °C with 220 rpm overnight. The following day 200 μ L of preinoculum was transferred into 4 mL of LB liquid media (with antibiotics) and cultured at 37 °C until the optical density at 600 nm ($OD_{600\text{ nm}}$) reached approximately 0.6. Then isopropyl- β -D-thiogalactopyranoside (IPTG) was added at a final concentration of 1 mM and the

culture was incubated at 30 °C for 20 h. The cells ($\sim 5 \times 10^8$ cells) were harvested by centrifugation, washed with 1 mL of phosphate buffer (pH 7.0) and then resuspended in 100 μ L of phosphate buffer. The recombinant protein was released by following six cycles of the freeze–thaw method and checked by SDS-PAGE (ESI Fig. S1†). For freeze–thaw cycles, the cell



suspension in phosphate buffer was frozen in a dry ice and isopropanol bath for 5 min and thawed in a 37 °C water bath.

For whole-cell biotransformation, after IPTG induction the culture was incubated at 30 °C for 5 h to increase biomass. The cell pellet was collected by centrifugation and resuspended in M9 minimal medium (resulting in an OD_{600 nm} of ~1.5) with 1 mM of IPTG. The culture broth was aliquoted (500 µL in each well) in the 96-deep-well plate (VWR, Denmark) and supplemented with tryptophan and tyrosine (0.5 mM or 1 mM of each). The plate was then incubated at 30 °C and 300 rpm for 5 days. The culture broth was extracted with an equal volume of methanol for high performance liquid chromatography (HPLC) and electrospray ionization mass analysis.

To calculate dry cell weight (DCW) of the *E. coli* recombinant strains, the cell pellets were collected in a pre-weighed Eppendorf tube by centrifuging 1 ml of culture broth (combining samples from two wells) at 6000g for 10 min. Then the cell pellets were dried at 60 °C in a vacuum oven until a constant weight was obtained. The cell pellets were used to determine the DCW as the biomass. Triplicate reading was carried out.

Product analysis and quantification

The bioconversion products from *E. coli* recombinant strains were analyzed and quantified by HPLC (Ultimate 3000, Thermo Scientific, USA) equipped with a Discovery® HS F5 column (4.6 × 150 mm, 5.0 µM particle size, Supelco, Sigma-Aldrich) connected to a UV detector (260 nm, 290 nm, 360 nm and 370 nm). A flow rate of 0.5 mL min⁻¹ was used with a linear gradient of 10 mM ammonium formate buffer (pH 3 adjusted with formic acid) (Phase A) and acetonitrile (Phase B) by the following method: 0–3 min (25% B), 3–15 min (25–75% B), 15–25 min (75% B), and 25–29 min (75–25% B) and 29–30 min (25% B). For quantification of metabolites, calibration curves of purified compounds were drawn using 6.25, 12.5, 25, and 50 µg mL⁻¹ concentrations. The exact mass of the compounds were analyzed by using Orbitrap Fusion (Thermo Scientific, USA) with a Dionex 3000 RX HPLC system (Thermo Scientific, USA) in the positive and negative ion modes.

Structural elucidation

The recombinant strain *E. coli* SM4 (*E. coli* BL21(DE3) harboring *scyA*, *scyB*, *scyC*, *scyD*, *scyE*, *scyF*, *tyrP* and *dsbA*) was cultured in 1 L of M9 minimal media. During induction by IPTG, 500 µM of tryptophan and tyrosine were also supplemented and after 5 days of incubation, the isolation process of the biotransformation product was undertaken. The culture broth was centrifuged at 6800g for 12 min to separate supernatant and cell pellet. Then the supernatant was extracted with an equal volume of ethyl acetate whereas the cell pellet was extracted with 100 mL of an ethyl acetate and acetone (3 : 1) mixture. The organic phase was collected and concentrated to dryness by evaporation of excess solvent. The remaining products were dissolved in methanol and the isolated crude extracts from supernatant and cell pellet were combined. The

extracted crude compound was chromatographed on PREP-HPLC (Ultimate 3000, Thermo Scientific, USA) under the following conditions: column, Discovery® HS F5 (4.6 × 150 mm, 5.0 µM particle size, Supelco, Sigma-Aldrich); UV detection, 290 nm; flow rate, 1.0 mL min⁻¹; under similar gradient conditions of solvents as mentioned above. The fractions were collected and the purified fractions were completely dried in a SpeedVac concentrator (SAVANT SC210A, Thermo Scientific, USA). The structural elucidation of the purified compounds was done by NMR analysis (¹H, ¹³C, Correlation Spectroscopy (COSY), Heteronuclear Single Quantum Coherence (HSQC), Heteronuclear multiple-bond correlation spectroscopy (HMBC)) and the relative stereochemistry for compound 4 was assigned from 1D-Nuclear Overhauser effect (NOE) experiment. The NMR analysis for structural elucidation of compounds 5, 6, 7, 8 and 9 are described in ESI.† NMR spectra were obtained in DMSO-d₆ (Aldrich, Chicago, IL, USA) using a Bruker Advance 600 instrument (600 MHz). For the ¹H-NMR experiment, 32 transients spectra were acquired with a spectral width of 8000 Hz. All NMR data were processed using XWINNMR (Bruker).

Results and discussion

Heterologous expression of the putative scytonemin gene cluster

Recent studies have shown that *N. punctiforme* genes have been well expressed and functional in *E. coli*.^{30,31} Accordingly, we chose to construct our recombinant pathway in *E. coli* using the native genes of *N. punctiforme*. For the expression of the putative scytonemin biosynthetic gene cluster, the recombinant plasmids pC-ScyABC-ScyDEF, pE-GtAroB-TrpEC and pA-TrpAB-TrpDU were constructed, and they were transformed into *E. coli* BL21 to create the strain *E. coli* STN. Upon IPTG induction, the cultures of *E. coli* expressing the putative scytonemin biosynthetic gene cluster (*E. coli* STN strain) in M9 minimal media turned yellow whereas the uninduced cultures did not have any color (data not shown). The metabolites produced by *E. coli* STN strain were analyzed by HPLC and mass analysis. The *E. coli* STN strain did not produce scytonemin upon IPTG induction. However, the monomer of scytonemin (compounds 4) and a new alkaloid derivative (compound 7) were produced as the dominant products from the endogenous amino acids (Fig. 3).

Despite the production of compound 4, the absence of scytonemin in the metabolites from STN was either due to the lack of dimerization enzyme(s) in the putative scytonemin gene cluster or inactive putative dimerization enzyme(s) during heterologous expression in *E. coli*. Genome analysis and comparison among several cyanobacterial strains for the conserved localization in the scytonemin clusters revealed a five-gene satellite cluster, oriented in the same transcriptional direction in *N. punctiforme*.¹⁵ Of five genes in the cluster, two genes are annotated as unknown hypothetical proteins, and three genes are annotated as putative metal-dependent hydro-



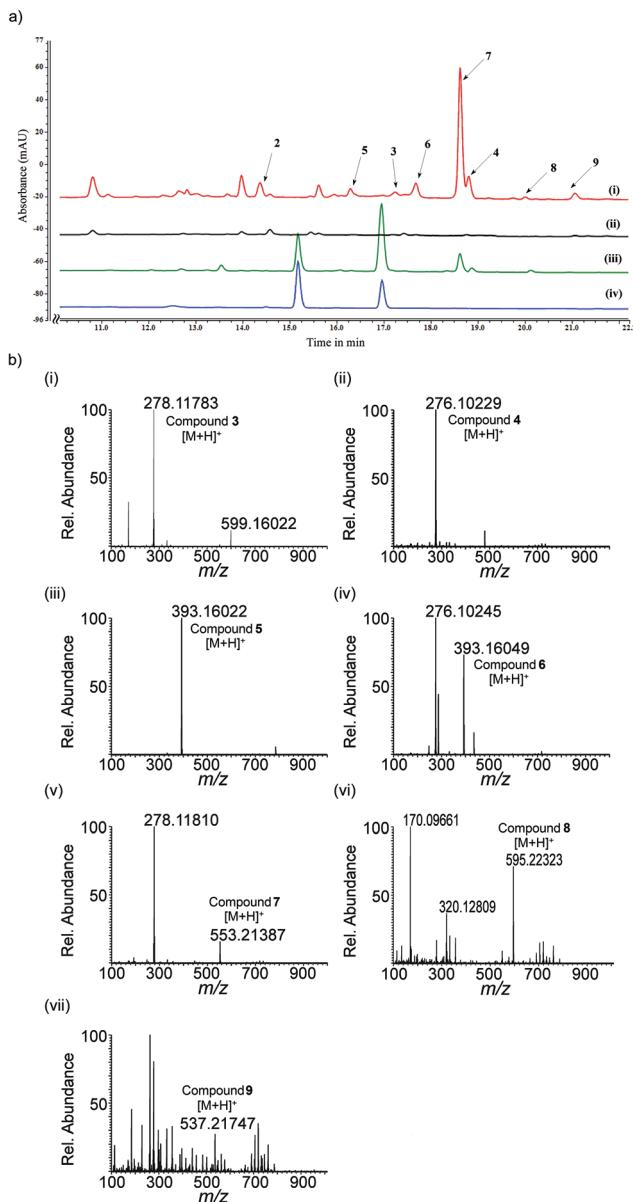


Fig. 3 (A) HPLC analysis of bioconversion products from *E. coli* SM4 and STN strains. (i) metabolites from *E. coli* SM4 supplemented with 1 mM of L-tryptophan and 1 mM of L-tyrosine, (ii) metabolites from *E. coli* SM4 without supplementation of substrates (control), (iii) metabolites from *E. coli* STN with IPTG induction, and (iv) metabolites from *E. coli* STN without IPTG induction (control). Compounds 2, 3, 4, 5, 6, 7, 8, and 9 have a retention time of 14.2, 17.3, 18.8, 16.1, 17.8, 18.6, 20.3 and 21.1 min, respectively. (B) LC/ESI-MS analysis of metabolites from *E. coli* SM4 in the positive mode: (i) exact mass of compound 3 $[M + H]^+$ $[m/z]$ (278.11783), (ii) exact mass of compound 4 $[M + H]^+$ $[m/z]$ (276.10229), (iii) exact mass of compound 5 $[M + H]^+$ $[m/z]$ (393.16022), (iv) exact mass of compound 6 $[M + H]^+$ $[m/z]$ (393.16049), (v) exact mass of compound 7 $[M + H]^+$ $[m/z]$ (553.21387), (vi) exact mass of compound 8 $[M + H]^+$ $[m/z]$ (595.22323), and (vii) exact mass of compound 9 $[M + H]^+$ $[m/z]$ (537.21747).

lase, putative prenyltransferase and putative type I phosphodiesterase. In addition, the transcriptional studies showed that all five genes in this cluster were upregulated under UV

irradiation.¹⁶ Hence, it was predicted that besides the putative gene cluster shown in Fig. 2, this satellite five-gene cluster might be involved during scytonemin biosynthesis. However, due to unclear annotations and lack of biochemical characterization, the role of this satellite cluster is still ambiguous.

Expression of structural core biosynthetic genes

Comparative genomic analysis of the scytonemin gene cluster from various cyanobacterial strains revealed that six gene products of ScyA-F are anticipated to produce the monomer moiety of scytonemin, and the final reaction, *i.e.*, dimerization step was predicted to catalyze by tyrosinase (TyrP) and/or oxidoreductase (DsbA) (Fig. 1).¹⁵ Accordingly, we constructed the recombinant plasmids pACYC-ScyB, pCDF-ScyAB, pRSF-ScyEF and pET-TyrP-DsbA and introduced them into *E. coli* BL21 (DE3). The resulting strain was designated as *E. coli* SM4. The *in vivo* isotope labeling studies in cyanobacterial strains showed that both labeled tryptophan and tyrosine were incorporated into the scytonemin structure during its biosynthesis.³² So, we supply tryptophan and tyrosine as precursor substrates during the biotransformation of *E. coli* SM4. The culture broth of *E. coli* SM4 strain supplemented with these precursors turned yellow and the yellowish product was primarily accumulated in the cell pellet (ESI Fig. S2†). HPLC and mass analysis of the bioconversion products of SM4 strain upon supplementation of 500 μ M of tryptophan and tyrosine accumulated compound 2 ($C_{18}H_{17}NO_3$ calculated $[M + H]^+$: 296.12866, found: 296.12876 and calculated $[M - H]^+$: 294.11301, found 294.11344), compound 3 ($C_{18}H_{15}NO_2$ calculated $[M + H]^+$: 278.11810, found: 278.11783), compound 4 ($C_{18}H_{13}NO_2$ calculated $[M + H]^+$: 276.10245, found: 276.10229) along with new alkaloid derivatives compound 5 ($C_{26}H_{20}N_2O_2$ calculated $[M + H]^+$: 393.16030, found: 393.16022), compound 6 ($C_{26}H_{20}N_2O_2$ calculated $[M + H]^+$: 393.16030, found: 393.16049), compound 7 ($C_{36}H_{28}N_2O_4$ calculated $[M + H]^+$: 553.21273, found: 553.21387), compound 8 ($C_{38}H_{30}N_2O_5$ calculated $[M + H]^+$: 595.22329, found: 595.22323) and compound 9 ($C_{36}H_{28}N_2O_3$ calculated $[M + H]^+$: 537.21781, found: 537.21747) (Fig. 3A and 3B and ESI Fig. S4†). All of these five new alkaloid derivatives have very similar UV-absorption spectra to that of compound 3 (ESI Fig. S3†). The structure of compounds 4, 6, 7, 8 and 9 was confirmed by NMR analysis (1H , ^{13}C , HSQC, HMBC) (Table 3, S1–S4 and ESI Fig. S5–S10†).

The absence of scytonemin in the bioconversion products of both SM4 and STN strains indicates that the final dimerization step is the major bottleneck in *E. coli*. Structural elucidation of the new alkaloid derivatives (shunt products) revealed that all five compounds were produced from the oxidation of intermediate compound 3, *i.e.*, either by the formation of C–C bond with indole or dimerization of compound 3. To gain more information about these new derivatives such as their synthetic origin and plausible bioactivities, we searched the literature to ascertain whether any of these compounds have been previously reported. An anti-inflammatory drug target I κ B kinase inhibitor, PS1145, and a proteasome inhibitor, Nostodione A, are structurally similar to the monomer moiety



Table 3 ^1H and ^{13}C -NMR signals of compound 4 (600 MHz, DMSO- d_6)

Position	Chemical shift (ppm)	
	^{13}C	^1H
1	204.85	
2	36.33	3.51, s
3 ^a	119.37	
4	139.98	
5	119.10	7.50, d ($J = 7.79$ Hz)
6	120.01	7.07, t ($J = 7.48$ Hz)
7	123.28	7.19, t ($J = 7.25$ Hz)
8	112.93	7.53, d ($J = 8.20$ Hz)
9	123.56	
10		10.93, s
11 ^a	139.69	
12	125.54	
13	124.34	6.98, s
14	125.78	
15	130.64	7.63, d ($J = 8.51$ Hz)
16	116.21	6.93, d ($J = 8.52$ Hz)
17	158.60	
18		10.03, s

^a Assignments of carbon 3 and 11 may be switched.

of scytonemin.³³ Nostodione A is generated upon ozonolysis of the reduced form of scytonemin,³⁴ and this compound has been isolated from *N. commune*³⁵ and a fresh water cyanobacterium, *Scytonema hofmanni*.³⁶ Similarly, the three new scytonemin derivatives, dimethoxyscytonemin, tetramethoxy-scytonemin and scytonin, have been identified from the organic extracts of *Scytonema* sp. These compounds do not possess cytotoxic effects even at 10 μM and also did not inhibit the growth of Gram positive, Gram negative and fungi at the concentration of 1 μM .³⁷ All of these previously reported derivatives are derived from the scytoneman skeleton of scytonemin. To the best of our knowledge, all the shunt products we found in this study have not been reported yet from any cyanobacterial strains including *N. punctiforme*. So, it is plausible that these shunt oxidation pathways are catalyzed by *E. coli* endogeneous enzyme(s) consuming the accumulated compound 3 in the cell.

Structural elucidation of compound 4

The ^1H and ^{13}C -NMR signals of compound 4 are given in Table 3 whereas the COSY, HMBC, HSQC and NEO spectrum are given in ESI (ESI Fig. S5†). In the ^1H -NMR spectrum, the low field singlet signals at 10.03 ppm and 10.93 ppm correspond to phenyl hydroxyl and indole amide groups, respectively, the signals between 7 ppm and 8 ppm correspond to typical aromatic phenyl and indole rings and the signal at 3.51 ppm corresponds to an aliphatic signal. The COSY spectrum confirmed the proton observations and revealed a correlation between the amide and one of the terminal protons of the indole proton system (4 bonds apart), allowing a sequential assignment of the proton spectrum (in fact this seems to be a 5 bond correlation from the NH to the opposite side of the indole proton network). The HSQC correlated these proton signals to their respective carbons, permitting the firm assign-

ment of all non-quaternary carbons. The HMBC allowed the assignment of some quaternary signals and the observation of a correlation between the aliphatic signal and a resonance at 204.85 ppm (only ketones resonate at this frequency). Due to the scarcity of protons in this molecule, the fact that HMBC signals can correlate to 2, 3 or 4 bonds apart and the cyclic nature of the molecule, sequential assignment and structural confirmation of the 5 membered ring becomes virtually impossible. The presence of an indole, a phenyl and a ketone group is indisputable, however their position could not be ascertained so six structures as shown in Fig. 4A were possible.

At this stage a NOE spectrum was acquired. The NOE spectrum revealed a correlation between the amide proton and signals of the phenyl group suggesting only possible structures (i) and (vi) in Fig. 4A. Also, a signal was observed between the aliphatic group and a proton on the indole ring but not with the phenyl ring and the amide group, which strongly suggests that the possible structure for compound 4 is structure (i) in

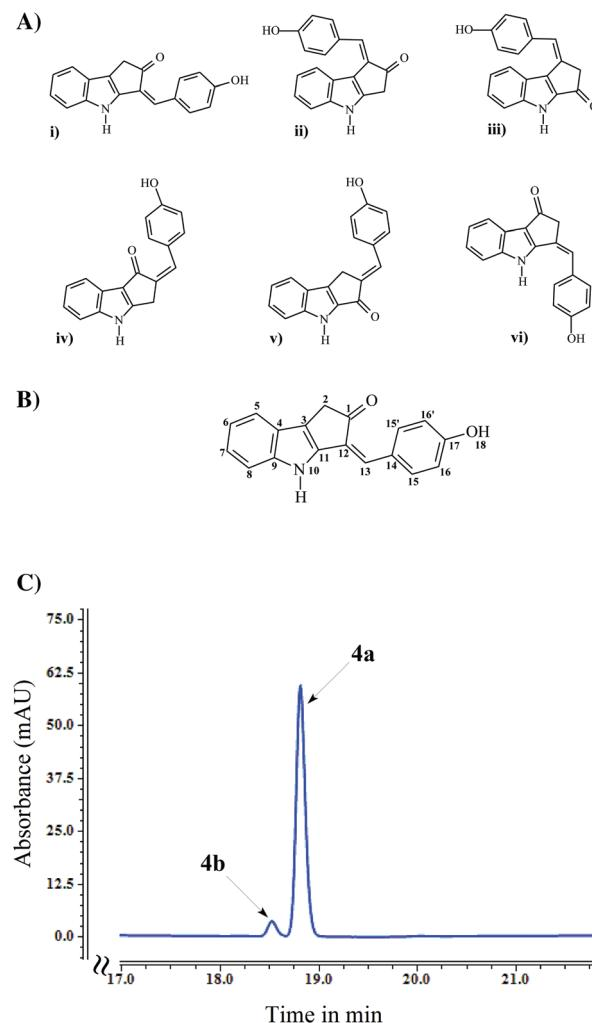


Fig. 4 (A) Six possible structures for compound 4 compatible with proton, carbon, COSY, HSQC and HMBC NMR analysis. (B) Structure of the compound 4 with atom numbering. (C) HPLC analysis of purified compound 4 from biotransformation of *E. coli* SM4 at 360 nm.



Fig. 4A. The confirmed structure of compound **4** along with atom numbering is given in Fig. 4B.

Although the NMR analysis confirmed structure **4a**, two isomeric forms *i.e.*, keto (**4a**) and enol (**4b**) forms are feasible structures for compound **4** as a result of keto–enol tautomerization. Owing to the lower energy, the keto form is thermodynamically more stable than the enol form, so the equilibrium heavily favors the formation of the keto form at room temperature.^{38,39} In addition, the equilibrium shifts toward the keto form in polar solvents mainly due to the involvement of lone pairs (present in oxygen of the keto group) in hydrogen bond formation with the solvent, making them less available to form hydrogen bonds with the enol form.^{40,41} HPLC chromatogram of the purified compound **4** contained two peaks: a major peak at a retention time of 18.8 min and a minor peak at 18.5 min retention time (Fig. 4C). Regardless of an absorbance maxima shifting (from 408 nm for major peak to 429 nm for minor peak), both of these compounds had very much similar UV absorbance spectra (ESI Fig. S3†). Hence, despite the formation of both keto and enol forms of compound **4**, only keto form (**4a**) was detected in NMR analysis.

Minimal genes for the production of the scytonemin monomer

To identify the minimal set of genes required for the production of the monomer moiety of scytonemin, a number of *E. coli* recombinant strains were constructed and their metabolites were analyzed following whole-cell biotransformation supplemented with tryptophan and tyrosine. First, the recombinant strain *E. coli* SM1 was constructed by introducing the plasmids pACYC-ScyB and pCDF-ScyA into *E. coli* BL21. Upon supplementation of tryptophan and tyrosine, this strain predominantly accumulated a decarboxylated product of intermediate **1** (*i.e.*, compounds **2a** or **2b**), which was detected by HPLC at 14.2 min retention time and identified by mass analysis (ESI Fig. S4†). Unlike the yellowish culture broth of SM4, the culture broth of SM1 supplemented with tryptophan and tyrosine was similar to the control strain (ESI Fig. S2†).

We then constructed the recombinant *E. coli* strains SM2 (*E. coli* BL21 harboring pACYC-ScyB and pCDF-ScyAC) and SM3 (*E. coli* BL21 harboring pACYC-ScyB, pCDF-ScyACD and pRSF-ScyEF). The biotransformation products of these strains were analyzed by exogenously supplying tryptophan and tyrosine. The culture broth of SM2 and SM3 strains is similar to that of the SM4, and both of these strains accumulated compound **4**, along with all five shunt products (compounds **5**, **6**, **7**, **8**, and **9**).

The *in vitro* characterization of the early biosynthetic enzymes of the scytonemin gene cluster proved that ScyB converts L-tryptophan to indole-3-pyruvic acid, which is coupled with *p*-hydroxyphenylpyruvic acid in the presence of ScyA to produce a labile β -keto acid adduct **1**.⁴² The endogenous *E. coli* enzyme, TyrB, catalyzes deamination of tyrosine providing one of the substrates, *p*-hydroxyphenylpyruvic acid, for ScyA.⁴³ However, in the absence of ScyC, the adduct **1** undergoes a facile, non-enzymatic decarboxylation to produce the

regioisomers **2a** and **2b**.⁴⁴ On the other hand, in the presence of ScyC, this non-enzymatic decarboxylation reaction is suppressed in favor of an intramolecular cyclization followed by dehydration and irreversible decarboxylation to produce compound **3a**.⁴⁴ Although the *in vitro* studies on scyC only accumulated **3a**,⁴⁴ we found that *in vivo* production of a monomer moiety of scytonemin (compound **4**) in *E. coli* can be achieved by expression of only three genes, scyABC, from *N. punctiforme*. This indicates that the endogenous enzyme(s) from the *E. coli* host catalyze the oxidation reaction to convert compound **3** into compound **4**. Furthermore, the dimerization reaction for the generation of compounds **7**, **8** and **9** are also likely catalyzed by the *E. coli* endogenous enzyme(s) instead of TyrP/DsbA from *N. punctiforme* as all five shunt products were also accumulated in the SM2 strain harboring only scyABC genes.

Comparison of compounds **4** and **7** yields

The production of the monomer moiety of scytonemin **4** and shunt dimer compound **7** from *E. coli* strains SM2 and SM4 was analyzed by supplementing tryptophan and tyrosine in M9 minimal medium at 5 days of reaction time. Utilizing endogenous tryptophan and tyrosine, the strains can produce compounds **4** and **7** upon IPTG induction. However, the yields of these compounds are higher upon supplementation of tryptophan and tyrosine. The biotransformation of strain SM2 supplemented with 500 μ M of substrates produced 5.0 mg L⁻¹ of compound **4** and 46.9 mg L⁻¹ of compound **7** whereas at 1 mM of substrate supplementation 7.3 mg L⁻¹ of compound **4** and 77.0 mg L⁻¹ of compound **7** were produced. Likewise, the strain SM4 produced 6.1 mg L⁻¹ of compound **4** and 46.3 mg L⁻¹ of compound **7** at 500 μ M substrate supplementation whereas at 1 mM of substrate supplementation 8.9 mg L⁻¹ of compound **4** and 87.1 mg L⁻¹ of compound **7** were produced (Fig. 5). On the other hand, upon IPTG induction the strain STN produced 4.2 mg L⁻¹ of compound **4** and 39.2 mg L⁻¹ of compound **7**, respectively, in M9 minimal media at 5 days.

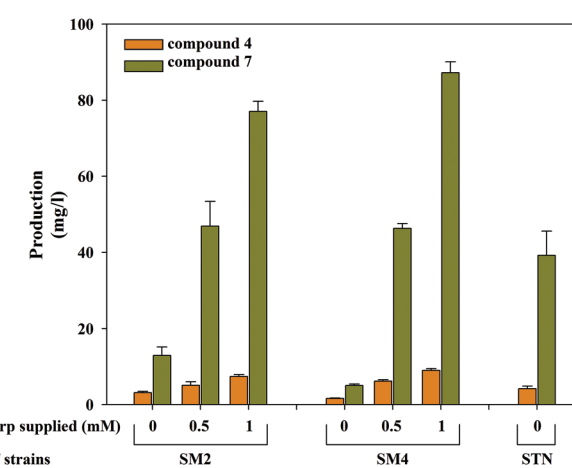


Fig. 5 Production of compounds **4** and **7** by *E. coli* recombinant strains SM2 and SM4 with/without supplementation of tryptophan and tyrosine and strain STN with/without IPTG induction.



The biomass (DCW) of IPTG induced substrate supplemented (1 mM of each) SM2 and SM4 strains were 1.84 g L⁻¹ and 1.94 g L⁻¹ at 5 days whereas those of the control strains were 1.87 g L⁻¹ and 1.81 g L⁻¹, respectively. Similarly, upon IPTG induction STN strain had 1.70 g L⁻¹ of DCW, whereas in the absence of induction this strain had 1.86 g L⁻¹ of DCW at 5 days. This showed the yield of 2.46 µg mg⁻¹ DCW, 3.96 µg mg⁻¹ DCW, and 4.56 µg mg⁻¹ DCW of the compound 4 by STN, SM2 and SM4 strains, respectively.

Conclusions

Following our work, the final dimerization step remains a major hurdle for the complete production of scytonemin in *E. coli*. Yet commercially, many drugs such as an anticancer drug, paclitaxel (Taxol),⁴⁵ and an antimalarial drug, artemisinin⁴⁶ have been produced by combining the biosynthetic and chemical synthetic approaches, highlighting the advantageous features of the bio-chemical approach for production of complex compounds. Our construction of a cell factory producing the monomer moiety of scytonemin could facilitate such production when combined with the already described chemosynthetic dimerization step.

Upon supplementation of 1 mM of tryptophan and tyrosine, *ca.* 158 µM of compound 7 (*i.e.*, 316 µM of the equivalent substrate concentration), *ca.* 32 µM of the monomer moiety of scytonemin, and comparable amounts of other derivatives (compounds 2, 3, 5, 6, 8, and 9) to that of compound 4 were produced. This indicates that nearly half of the supplemented substrates were utilized by the heterologously expressed scytonemin pathway in the constructed *E. coli* strain. This *E. coli* cell factory has a 3.5 fold higher yield of the scytonemin monomer moiety as compared to the scytonemin produced by the native producer *N. punctiforme*. Accordingly, our work represents an important milestone towards a green scytonemin process. However, the industrial applicability of this system requires a maximal conversion of substrates into the targeted product without (or low) the production of side products. Several techniques could possibly be applied for further optimization of this strain and biotransformation systems to enhance production. For example, inactivation of the targeted gene(s) could facilitate the production yields by preventing metabolic flux through undesired branch pathways.^{47,48} Furthermore, expression level optimizations of heterologous pathway enzymes could be achieved by altering the plasmid copy number⁴⁹ and promoter strength⁵⁰ and engineering the ribosome binding sites (RBS).⁵¹ Similarly, adaptive laboratory evolution (ALE) strategies have been broadly applied in metabolic engineering of *E. coli* for improving fitness, yield, production rate and cost-effectiveness. The ALE techniques are greatly effective for non-native pathway optimization which allows the selection of beneficial mutations in the production strains in an unbiased fashion.⁵² Likewise, immobilization of enzymes or whole cells has been successfully applied in numerous scientific and industrial processes.⁵³ Enzyme

properties such as stability, activity, specificity, selectivity, *etc.* have been greatly improved by enzyme immobilization and multi-enzyme co-localization.^{54,55} During biotransformation, supplementation of high substrate concentration may have a tendency to change the pH, osmotic pressure, *etc.* of culture media (or reaction conditions), thus limiting the bioconversion process. However, immobilization of the enzyme could increase resistance to such changes and it may also increase the enzyme concentration, which favors supplementation of higher substrate concentrations and hence increase the product yield. Immobilized technology has been extensively used in bioreactors for significant improvement of the yields in fermentation.⁵⁶ In addition, systematic and careful design in bioreactor and optimization of physical parameters such as cultivation conditions (temperature, dissolved oxygen and RPM), pH condition, media composition, *etc.* has a great impact in the bioconversion process.⁵⁷

Further in-depth studies to better understand the shunt pathway B is essential as a majority of compound 3 was consumed by this pathway. Likewise, compound 3 was also consumed by forming an adduct with the indole moiety through a shunt pathway A. Since tryptophanase is responsible for degradation of L-tryptophan into indole, pyruvate and ammonia,⁵⁸ the prevention of tryptophan degradation as well as the effect of shunt pathway A could be abolished by inactivation of chromosomal tryptophanase (*tnaA*) in *E. coli*. These strains could be further metabolically engineered for the overproduction of endogenous tryptophan and the tyrosine pool.^{59,60} For example, overexpression of branch pathway genes from chorismate to L-tyrosine and L-tryptophan can overproduce these amino acids.⁶¹ Hence, studies on the dimerization reaction for the complete synthesis of scytonemin in *E. coli* along with pathway optimizations to improve the yield of compound 4 will be the focus of future investigations.

Acknowledgements

This work was supported by Novo Nordisk Foundation. We are grateful to Prof. Søren Molin. We thank Dr Pedro Lamosa (ITQB, Portugal) for assistance with the NMR spectroscopic analyses and Dr Scott James Harrison for the MS analysis. We also thank Dr Hao Luo, Dr Jiangfeng Zhu and Dr Ariane Zutz for discussion during the manuscript preparation.

References

- 1 E. Leonard, W. Runguphan, S. O'Connor and K. J. Prather, *Nat. Chem. Biol.*, 2009, **5**, 292–300.
- 2 T. Hartmann, *Planta*, 2004, **219**, 1–4.
- 3 P. J. Proteau, W. H. Gerwick, F. Garcia-Pichel and R. Castenholz, *Experientia*, 1993, **49**, 825–829.
- 4 K. Strebhardt and A. Ullrich, *Nat. Rev. Cancer*, 2006, **6**, 321–330.



5 F. A. Barr, H. H. Silljé and E. A. Nigg, *Nat. Rev. Mol. Cell Biol.*, 2004, **5**, 429–440.

6 Y. Ito, H. Yoshida, F. Matsuzuka, N. Matsuura, Y. Nakamura, H. Nakamine, K. Kakudo, K. Kuma and A. Miyauchi, *Anticancer Res.*, 2004, **24**, 259–263.

7 G. Zhang, Z. Zhang and Z. Liu, *Tumour Biol.*, 2013, **34**, 1887–1894.

8 G. Zhang, Z. Zhang and Z. Liu, *Tumour Biol.*, 2013, **34**, 2241–2247.

9 C. S. Stevenson, E. A. Capper, A. K. Roshak, B. Marquez, C. Eichman, J. R. Jackson, M. Mattern, W. H. Gerwick, R. S. Jacobs and L. A. Marshall, *J. Pharmacol. Exp. Ther.*, 2002, **303**, 858–866.

10 C. S. Stevenson, E. A. Capper, A. K. Roshak, B. Marquez, K. Grace, W. H. Gerwick, R. S. Jacobs and L. A. Marshall, *Inflamm. Res.*, 2002, **51**, 112–114.

11 F. Garcia-Pichel, N. D. Sherry and R. W. Castenholz, *Photochem. Photobiol.*, 1992, **56**, 17–23.

12 K. Matsui, E. Nazifi, Y. Hirai, N. Wada, S. Matsugo and T. Sakamoto, *J. Gen. Appl. Microbiol.*, 2012, **58**, 137–144.

13 J. G. Dillon, C. M. Tatsumi, P. G. Tandingan and R. W. Castenholz, *Arch. Microbiol.*, 2002, **177**, 322–331.

14 C. M. Sorrels, P. J. Proteau and W. H. Gerwick, *Appl. Environ. Microbiol.*, 2009, **75**, 4861–4869.

15 T. Soule, K. Palmer, Q. Gao, R. M. Potrafka, V. Stout and F. Garcia-Pichel, *BMC Genomics*, 2009, **10**, 336–345.

16 T. Soule, F. Garcia-Pichel and V. Stout, *J. Bacteriol.*, 2009, **191**, 4639–4646.

17 T. Sakamoto, K. Kumihashi, S. Kunita, T. Masaura, K. Inoue-Sakamoto and M. Yamaguchi, *FEMS Microbiol. Ecol.*, 2011, **77**, 385–394.

18 A. Ekebergh, I. Karlsson, R. Mete, Y. Pan, A. Börje and J. M. Årtensson, *Org. Lett.*, 2011, **13**, 4458–4461.

19 A. Nakagawa, H. Minami, J. S. Kim, T. Koyanagi, T. Katayama, F. Sato and H. Kumagai, *Nat. Commun.*, 2011, **2**, 326.

20 J. Du, Z. Shao and H. Zhao, *J. Ind. Microbiol. Biotechnol.*, 2011, **38**, 873–890.

21 S. Y. Lee, D. Mattanovich and A. Villaverde, *Microb. Cell Fact.*, 2012, **11**, 156.

22 C. D. Murphy, *Org. Biomol. Chem.*, 2012, **10**, 1949–1957.

23 E. Matsumura, M. Matsuda, F. Sato and H. Minami, *Natural Products*, Springer, Berlin Heidelberg, 2013.

24 D. P. Clark, *FEMS Microbiol. Rev.*, 1989, **5**, 223–234.

25 S. Malla, M. A. Koffas, R. J. Kazlauskas and B. G. Kim, *Appl. Environ. Microbiol.*, 2012, **78**, 684–694.

26 B. Kim, H. Park, D. Na and S. Y. Lee, *Biotechnol. J.*, 2013, DOI: 10.1002/biot.201300263.

27 W. Chu, T. R. Zere, M. M. Weber, T. K. Wood, M. Whiteley, B. Hidalgo-Romano, E. Valenzuela Jr. and R. J. McLean, *Appl. Environ. Microbiol.*, 2012, **78**, 411–419.

28 G. Li and K. D. Young, *Microbiology*, 2013, **159**, 402–410.

29 J. Sambrook and D. W. Russell, *Molecular Cloning: A Laboratory Manual*, Cold Spring Harbor Laboratory Press, Cold Spring Harbor, NY, 3rd edn, 2001.

30 K. Koketsu, S. Mitsuhashi and K. Tabata, *Appl. Environ. Microbiol.*, 2013, **79**, 2201–2208.

31 Q. Gao and F. Garcia-Pichel, *J. Bacteriol.*, 2011, **193**, 5923–5928.

32 C. S. Jones, E. Esquenazi, P. C. Dorrestein and W. H. Gerwick, *Bioorg. Med. Chem.*, 2011, **19**, 6620–6627.

33 B. Haefner, *Drug Discovery Today*, 2003, **8**, 536–544.

34 P. J. Proteau, W. H. Gerwick, F. Garcia-Pichel and R. Castenholz, *Experientia*, 1993, **49**, 825–829.

35 A. Kobayashi, S. I. Kajiyama, K. Inawaka, H. Kanzaki and K. Z. Kawazu, *Z. Naturforsch., C: Biosci.*, 1994, **49**, 464–470.

36 S. H. Shim, G. Chlipala and J. Orjala, *J. Microbiol. Biotechnol.*, 2008, **18**, 1655–1658.

37 V. Bultel-Poncée, F. Felix-Theodore, C. Sarthou, J. F. Ponge and B. Bodo, *J. Nat. Prod.*, 2004, **67**, 678–681.

38 A. J. Kresge, *Pure Appl. Chem.*, 1991, **63**, 213–221.

39 B. Capon, *The Chemistry of Enols*, ed. Z. Rappoport, Wiley, NY, 1990.

40 S. G. Mills and P. J. Beak, *Org. Chem.*, 1995, **50**, 1216–1224.

41 W. Blokzijl, J. B. F. N. Engbert and M. J. Blandamer, *J. Chem. Soc., Perkin Trans. 2*, 1994, 455–458.

42 E. P. Balskus and C. T. Walsh, *J. Am. Chem. Soc.*, 2008, **130**, 15260–15261.

43 I. G. Fotheringham, S. A. Dacey, P. P. Taylor, T. J. Smith, M. G. Hunter, M. E. Finlay, S. B. Primrose, D. M. Parker and R. M. Edwards, *Biochem. J.*, 1986, **234**, 593–604.

44 E. P. Balskus and C. T. Walsh, *J. Am. Chem. Soc.*, 2009, **131**, 14648–14649.

45 C. McNeil, *J. Natl. Cancer Inst.*, 1995, **87**, 1106–1108.

46 C. J. Paddon, P. J. Westfall, D. J. Pitera, K. Benjamin, K. Fisher, D. McPhee, M. D. Leavell, A. Tai, A. Main, D. Eng, D. R. Polichuk, K. H. Teoh, D. W. Reed, T. Treynor, J. Lenihan, M. Fleck, S. Bajad, G. Dang, D. Dengrove, D. Diola, G. Dorin, K. W. Ellens, S. Fickes, J. Galazzo, S. P. Gaucher, T. Geistlinger, R. Henry, M. Hepp, T. Horning, T. Iqbal, H. Jiang, L. Kizer, B. Lieu, D. Melis, N. Moss, R. Regentin, S. Secret, H. Tsuruta, R. Vazquez, L. F. Westblade, L. Xu, M. Yu, Y. Zhang, L. Zhao, J. Lievense, P. S. Covello, J. D. Keasling, K. K. Reiling, N. S. Renninger and J. D. Newman, *Nature*, 2013, **496**, 528–532.

47 S. Malla, R. P. Pandey, B. G. Kim and J. K. Sohng, *Biotechnol. Bioeng.*, 2013, **110**, 2525–2535.

48 Z. L. Fowler, W. W. Gikandi and M. A. Koffas, *Appl. Environ. Microbiol.*, 2009, **75**, 5831–5839.

49 E. Chaignat, E. A. Yahya-Graison, C. N. Henrichsen, J. Chrast, F. Schütz, S. Pradervand and A. Reymond, *Genome Res.*, 2011, **21**, 106–113.

50 Z. Shao, G. Rao, C. Li, Z. Abil, Y. Luo and H. Zhao, *ACS Synth. Biol.*, 2013, **15**, 662–669.

51 N. R. Sandova, J. Y. Kim, T. Y. Glebes, P. J. Reeder, H. R. Aucoin, J. R. Warner and R. T. Gill, *Proc. Natl. Acad. Sci. U. S. A.*, 2012, **109**, 10540–10545.

52 V. A. Portnoy, D. Bezdan and K. Zengler, *Curr. Opin. Biotechnol.*, 2011, **22**, 590–594.



53 M. B. Cassidy, H. Lee and J. T. Trevors, *J. Ind. Microbiol.*, 1996, **16**, 79–101.

54 F. Jia, B. Narasimhan and S. Mallapragada, *Biotechnol. Bioeng.*, 2013, DOI: 10.1002/bit.25136.

55 C. Mateo, J. M. Palomo, G. Fernandez-Lorente, J. M. Guisan and R. Fernandez-Lafuente, *Enzyme Microb. Technol.*, 2007, **40**, 1451–1463.

56 P. Brodelius and J. Vandamme, *Biotechnology: A Comprehensive Treatise in Eight Volumes*, ed. J. F. Kennedy, VCH Verlagsgesellschaft mbH, Germany, 1987, vol. 7a.

57 F. R. Schmidt, *Appl. Microbiol. Biotechnol.*, 2005, **68**, 425–435.

58 M. N. Kazarinoff and E. E. Snell, *J. Biol. Chem.*, 1977, **252**, 7598–7602.

59 D. Juminaga, E. E. Baidoo, A. M. Redding-Johanson, T. S. Batth, H. Burd, A. Mukhopadhyay, C. J. Petzold and J. D. Keasling, *Appl. Environ. Microbiol.*, 2012, **78**, 89–98.

60 M. I. Chávez-Béjar, A. R. Lara, H. López, G. Hernández-Chávez, A. Martínez, O. T. Ramírez, F. Bolívar and G. Gosset, *Appl. Environ. Microbiol.*, 2008, **74**, 3284–3290.

61 M. Ikeda, *Appl. Microbiol. Biotechnol.*, 2006, **69**, 615–626.

